Space-Time Coded OTFS Modulation in High-Doppler Channels

Rose Mary Augustine, G. D. Surabhi, and A. Chockalingam
Department of ECE, Indian Institute of Science, Bangalore 560012

***Abstract*—Orthogonal time frequency space (OTFS) modulation is a 2-dimensional modulation technique designed in *delay-Doppler domain*, specially suited for doubly-dispersive fading channels. OTFS modulation uses additional transform operations at the transmitter and receiver on top of conventional multicarrier modulation operations, and is shown to achieve superior performance compared to OFDM in high-Doppler channels. It has been shown in the recent literature that the asymptotic diversity order of OTFS modulation is one. Also, OTFS with phase rotation using transcendental numbers has been shown to achieve full diversity in the delay-Doppler domain. In this paper, for the first time in the literature, we propose and investigate the use of space-time coding (STC) in OTFS modulation in a MIMO setting. We use the structure of Alamouti code, generalized to matrices, to achieve full transmit diversity in OTFS. We also show that the use of STC-OTFS along with phase rotation can achieve full diversity in both spatial and delay-Doppler domains. Also, STC-OTFS with phase rotation is found to achieve good diversity performance even with small frame sizes making it suited for low-latency applications.**

Keywords – *OTFS modulation, delay-Doppler domain, space-time coding, STC-OTFS, full diversity.*

I. Introduction

Wireless communication systems in the fifth generation and beyond are envisaged to operate in high-Doppler environments such as V2X communications, high speed trains, and mmWave communications, where the systems should be capable of providing high reliability and throughput in rapidly changing channel environments. The channel fading in such scenarios is often doubly dispersive in nature with high Dopplers. Orthogonal time frequency space (OTFS) modulation is a promising physical layer multiplexing technique that can achieve superior error performances compared to conventional multicarrier systems (such as OFDM) in such high-Doppler channels [1]-[7]. A key feature that differentiates OTFS modulation from other conventional modulation schemes is that information symbols in OTFS are multiplexed in the delay-Doppler domain, whereas they are multiplexed in the time-frequency domain in conventional modulation schemes. An advantage of signaling in the delay-Doppler domain is that a channel rapidly varying in time manifests as an almost invariant channel when viewed in the delay-Doppler domain. This relatively constant channel gain experienced by all the symbols in an OTFS transmission frame can greatly simplify the design of equalizer and reduce the overhead on the channel estimation in rapidly time-varying channels.

OTFS modulation was first proposed in [1] and was shown to achieve significantly better error performances compared to OFDM for vehicle speeds ranging from 30 kmph to 500 kmph in 4 GHz band [1]-[3]. OTFS is also shown to perform well in 28 GHz mmWave frequency band where Dopplers can be quite high even for low/moderate vehicle speeds because of the high carrier frequencies involved [4]. OTFS modulation architected over the conventional OFDM has been considered in [5]. The performance of OTFS with low-complexity detection algorithms has been investigated in [6],[7]. Low-complexity signal detection and channel estimation aspects in multiple-input multiple-output OTFS (MIMO-OTFS) systems have been explored in [8]. While [8] considered OTFS with multiple transmit antennas, it did not consider OTFS with space-time coding. A formal analysis of the asymptotic diversity order of OTFS is presented in [9], where it has been shown that the asymptotic diversity order of OTFS (as SNR $\rightarrow \infty$) is one. Further, potential for higher diversity orders in the finite SNR regime for large OTFS frame sizes has been pointed out in [9]. Also, [9] presents a phase rotation scheme for OTFS that uses transcendental numbers and extracts the full diversity offered by the delay-Doppler channel.

In this paper, for the first time in the emerging OTFS literature, we explore the possibility of extracting full diversity in both spatial as well as delay-Doppler domains in OTFS using space-time coding (STC). Specifically, since OTFS is a 2D modulation, we extend the well-known Alamouti code structure to a matrix form in OTFS and propose a STC-OTFS scheme. We show that the proposed STC-OTFS system can achieve full spatial diversity. Next, we propose the use STC-OTFS along with a phase rotation scheme and show that the proposed STC-OTFS with phase rotation can achieve full spatial and delay-Doppler diversity. This scheme is simple and attractive for low-latency systems which use small frame sizes for low decoding delays.

The rest of the paper is organized as follows. The OTFS modulation in SISO and MIMO settings is presented in Sec. II. The proposed STC-OTFS scheme, diversity analysis, and phase rotation scheme are presented in Sec. III. Simulation results and discussions are presented in Sec. IV. Conclusions are presented in Sec. V.

II. OTFS Modulation

The basic premise in OTFS modulation is the use of delay-Doppler domain for multiplexing the modulation symbols. The block diagram for OTFS modulation scheme is shown in Fig. 1. The inner box in the block diagram can be any multicarrier time-frequency (TF) modulation and the outer box with pre- and post-processor constitutes the OTFS modulator.

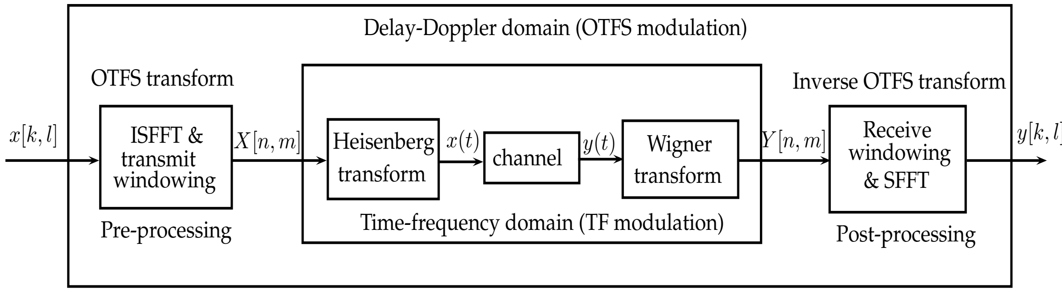

Fig. 1: OTFS modulation scheme.

A. Time-frequency modulation

- The TF plane is sampled at intervals T and Δf, respectively, to obtain a 2D grid Λ, which is defined as
$$\Lambda = \{(nT, m\Delta f), n = 0, \cdots, N-1, m = 0, \cdots, M-1\}. \tag{1}$$
- The signal in TF domain $X[n,m]$, $n = 0, \cdots, N-1$, $m = 0, \cdots, M-1$ in a given packet burst has duration NT and occupies a bandwidth of $M\Delta f$.
- Transmit and receive pulses $g_{tx}(t)$ and $g_{rx}(t)$, respectively, which are assumed to be bi-orthogonal are used. The TF signal $X[n,m]$ is transformed to the time domain signal $x(t)$ through Heisenberg transform, given by
$$x(t) = \sum_{n=0}^{N-1} \sum_{m=0}^{M-1} X[n,m] g_{tx}(t - nT) e^{j2\pi m \Delta f (t - nT)}. \tag{2}$$
- At the receiver, the received signal is matched filtered with the pulse $g_{rx}(t)$, yielding the cross-ambiguity function $A_{g_{rx},y}(\tau, \nu)$. Sampling this function on the lattice Λ yields the matched filter output, given by
$$Y[n,m] = A_{g_{rx},y}(\tau,\nu)|_{\tau=nT, \nu=m\Delta f}. \tag{3}$$
- If the complex baseband channel impulse response $h(\tau,\nu)$ has finite support bounded by $(\tau_{\max}, \nu_{\max})$, the relation between $Y[n,m]$ and $X[n,m]$ for TF modulation is given by [3]
$$Y[n,m] = H[n,m]X[n,m] + V[n,m], \tag{4}$$
where $V[n,m]$ is additive white Gaussian noise and $H[n,m]$ is given by
$$H[n,m] = \int_\tau \int_\nu h(\tau,\nu) e^{j2\pi\nu nT} e^{-j2\pi(\nu + m\Delta f)\tau} \mathrm{d}\nu \mathrm{d}\tau. \tag{5}$$

B. OTFS modulation

- The information symbols in the delay-Doppler domain $x[k,l]$ are mapped to TF domain symbols $X[n,m]$ as
$$X[n,m] = \frac{1}{MN} \sum_{k=0}^{N-1} \sum_{l=0}^{M-1} x[k,l] e^{j2\pi\left(\frac{nk}{N} - \frac{ml}{M}\right)}. \tag{6}$$
- $X[n,m]$ is then TF modulated as described in the previous subsection for transmission through the channel. The received signal $y(t)$ is transformed into $Y[n,m]$ using Wigner filter as described by (3).
- $Y[n,m]$ is then converted from TF domain to delay-Doppler domain to obtain $y[k,l]$ as
$$y[k,l] = \frac{1}{MN} \sum_{k=0}^{N-1} \sum_{l=0}^{M-1} Y[n,m] e^{-j2\pi\left(\frac{nk}{N} - \frac{ml}{M}\right)}. \tag{7}$$

C. Input-output relation in OTFS

Consider a baseband delay-Doppler channel $h(\tau,\nu)$ with P taps or P clusters of reflectors, each associated with a delay τ_i, a Doppler ν_i and a fade coefficient h_i. Using (2) through (7), the input-output relation for the P path channel (assuming rectangular transmit and receive window functions) is given by [6]
$$y[k,l] = \sum_{i=1}^{P} h'_i x[(k - \beta_i)_N, (l - \alpha_i)_M)] + v[k,l], \tag{8}$$
where h'_is are given by
$$h'_i = h_i e^{-j2\pi\nu_i\tau_i}, \tag{9}$$
α_i and β_i are assumed to be integers and they denote the indices of the delay tap and Doppler frequency tap corresponding to τ_i and ν_i, respectively ($\tau_i \triangleq \frac{\alpha_i}{M\Delta f}$ and $\nu_i \triangleq \frac{\beta_i}{NT}$), and $v[k,l]$ denotes the additive white Gaussian noise. It is assumed that the h_is are i.i.d and are distributed as $\mathcal{CN}(0, 1/P)$, assuming uniform scattering profile. Denoting the $N \times M$ delay-Doppler channel grid with $\widehat{\mathbf{H}}$, the (k,l)th entry of $\widehat{\mathbf{H}}$, denoted by $\hat{h}[k,l]$ is defined as
$$\hat{h}[k,l] = \begin{cases} h'_i & \text{if } k = \beta_i \ \& \ l = \alpha_i \text{ for some } i \in \{1, \cdots, P\} \\ 0 & \text{otherwise.} \end{cases} \tag{10}$$
Now, the input-output relation in (8) can be vectorized as [6]
$$\mathbf{y} = \mathbf{H}\mathbf{x} + \mathbf{v}, \tag{11}$$
where $x_{k+Nl} = x[k,l]$, $y_{k+Nl} = y[k,l]$, $v_{k+Nl} = v[k,l]$, $k = 0, \cdots, N-1$, $l = 0, \cdots, M-1$, and $\mathbf{H}$ is an $MN \times MN$ matrix whose jth row ($j = k + Nl$, $j = 0, 1, \cdots, MN-1$), denoted by $\mathbf{H}[j]$, is given by
$$\mathbf{H}[j] = [\hat{h}[(k-0)_N, (l-0)_M] \ \hat{h}[(k-1)_N, (l-0)_M] \ \cdots \ \hat{h}[(k-(N-1))_N, (l-(M-1))_M]]. \tag{12}$$
Note that, due to the modulo operations in (12), each row and each column of $\mathbf{H}$ have only P non-zero elements.

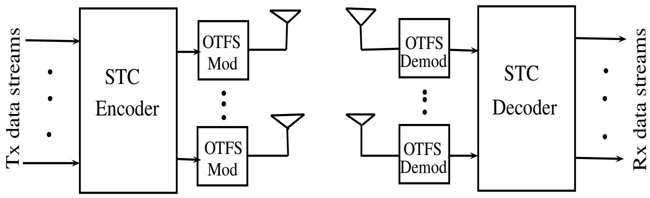

Fig. 2: STC-OTFS scheme.

D. MIMO-OTFS

For a MIMO-OTFS system with n_t transmit and n_r receive antennas, the linear vector channel in (11) can be extended and the input output relation can be written as [8]

$$\mathbf{y}_{\text{MIMO}} = \mathbf{H}_{\text{MIMO}}\mathbf{x}_{\text{MIMO}} + \mathbf{v}_{\text{MIMO}}, \tag{13}$$

where

$$\mathbf{H}_{\text{MIMO}} = \begin{bmatrix} \mathbf{H}_{11} & \mathbf{H}_{12} & \dots & \mathbf{H}_{1n_t} \\ \mathbf{H}_{21} & \mathbf{H}_{22} & \dots & \mathbf{H}_{2n_t} \\ \vdots & \vdots & \ddots & \vdots \\ \mathbf{H}_{n_r1} & \mathbf{H}_{n_r2} & \dots & \mathbf{H}_{n_rn_t} \end{bmatrix}, \tag{14}$$

$\mathbf{H}_{ij}$ denotes the $MN \times MN$ equivalent channel matrix between the jth transmit antenna and ith receive antenna, $\mathbf{x}_{\text{MIMO}} = [{\mathbf{x}_1}^T, {\mathbf{x}_2}^T, \cdots, {\mathbf{x}_{n_t}}^T]^T \in \mathbb{C}^{n_tNM\times 1}$ is the MIMO-OTFS transmit vector, $\mathbf{y}_{\text{MIMO}} = [{\mathbf{y}_1}^T, {\mathbf{y}_2}^T, \cdots, {\mathbf{y}_{n_t}}^T]^T \in \mathbb{C}^{n_tNM\times 1}$ is the MIMO-OTFS received vector, and $\mathbf{v}_{\text{MIMO}}$ is the noise vector.

III. Space-time coded OTFS

In this section, we present the STC-OTFS scheme. The block diagram of the STC-OTFS is shown in Fig. 2. We first introduce an alternate input-output relation for OTFS which is crucial for the construction of space-time code for OTFS. This representation also simplifies the diversity analysis of the space-time code.

A. An alternate input-output relation for OTFS

Consider the vectorized formulation of the input-output relation in OTFS given by (11). Recall from Sec. II-C that there are only P non-zero elements in each row and each column of the equivalent channel matrix $\mathbf{H}$ in (11). Also, it can be seen from (8) that each transmitted symbol experiences the same channel gain. Therefore, $\mathbf{H}$ has only P (which can be maximum up to MN) unique non-zero entries in it. With this, the vectorized input-output model in (11) can be written in an alternate form as

$$\mathbf{y}^T = \mathbf{h}'\mathbf{X} + \mathbf{v}^T, \tag{15}$$

where $\mathbf{y}^T$ is $1\times MN$ received vector, $\mathbf{h}'$ is $1\times MN$ vector with its $m = (k + Nl)$th entry given by $\mathbf{h}'_m = \hat{h}[k, l]$ and contains P non-zero elements, $\mathbf{v}^T$ is the $1 \times MN$ noise vector, and $\mathbf{X}$ is an $MN \times MN$ matrix whose ith column ($i = k + Nl$, $i = 0, 1, \cdots, MN - 1$), denoted by $\mathbf{X}[i]$, is given by

$$\mathbf{X}[i] = \begin{bmatrix} x_{(k-0)_N+N(l-0)_M} \\ x_{(k-1)_N+N(l-0)_M} \\ \vdots \\ x_{(k-(N-2))_N+N(l-(M-1))_M} \\ x_{(k-(N-1))_N+N(l-(M-1))_M} \end{bmatrix}. \tag{16}$$

The matrix $\mathbf{X}$ is an $MN \times MN$ matrix with $\mathbf{x}$ as its first row and the remaining rows being the permutations of $\mathbf{x}$. Also, $\mathbf{X}$ is a block circulant matrix with M circulant blocks, each of size $N \times N$. The extension of the alternate representation in (15) to MIMO-OTFS is straightforward and is crucial for space-time coding in OTFS. In the effective MIMO-OTFS channel matrix in (14), assuming each $\mathbf{H}_{ij}$ has only P unique entries (P tap channel), $\mathbf{H}_{\text{MIMO}}$ has Pn_tn_r unique entries. Further, each row of $\mathbf{H}_{\text{MIMO}}$ has only n_tP non-zero elements and each column has only n_rP non-zero elements. Following (15), the MIMO-OTFS system model in (13) can be written in an alternate form as

$$\begin{bmatrix} \mathbf{y}_1^T \\ \mathbf{y}_2^T \\ \vdots \\ \mathbf{y}_{n_r}^T \end{bmatrix} = \begin{bmatrix} \mathbf{h}'_{11} & \mathbf{h}'_{12} \cdots & \mathbf{h}'_{1n_t} \\ \mathbf{h}'_{21} & \mathbf{h}'_{22} \cdots & \mathbf{h}'_{2n_t} \\ \vdots & & \\ \mathbf{h}'_{n_r1} & \mathbf{h}'_{n_r2} \cdots & \mathbf{h}'_{n_rn_t} \end{bmatrix} \begin{bmatrix} \mathbf{X}_1 \\ \mathbf{X}_2 \\ \vdots \\ \mathbf{X}_{n_t} \end{bmatrix} + \begin{bmatrix} \mathbf{v}_1^T \\ \mathbf{v}_2^T \\ \vdots \\ \mathbf{v}_{n_r}^T \end{bmatrix}, \tag{17}$$

where $\mathbf{y}_i^T \in \mathbb{C}^{1\times MN}, i \in \{1, 2, \cdots, n_r\}$ is the received vector at the ith receive antenna, $\mathbf{X}_j \in \mathbb{C}^{MN\times MN}, j \in \{1, 2, \cdots, n_t\}$ is the symbol matrix corresponding to jth transmit antenna, and $\mathbf{h}'_{ij}$ is the $1 \times MN$ channel vector from jth transmit antenna to ith receive antenna, as defined in (15).

B. Encoding and decoding

Consider OTFS signaling over a $n_t \times n_r$ MIMO channel. We assume quasi-static delay-Doppler channel over T' frame duration, i.e., NTT' channel uses. A STC-OTFS codeword matrix can be defined as a block matrix $\tilde{\mathbf{X}}$ of size $n_tMN \times T'MN$, in which each block $\tilde{\mathbf{X}}_{kt}$ denotes $MN \times MN$ OTFS transmit matrix from the kth antenna in the tth frame use. If the space-time code matrix $\tilde{\mathbf{X}}$ contains Q independent OTFS symbol matrices which are transmitted over T' frame uses, then the rate of the code is Q/T' symbols per channel use. We consider a 2×1 system, and construct a space-time code using the Alamouti code structure [11], generalized to matrices [10]. This results in a rate-1 Alamouti STC-OTFS codeword matrix of size $2MN \times 2MN$ given by

$$\tilde{\mathbf{X}} = \begin{bmatrix} \mathbf{X}_1 & -\mathbf{X}_2^H \\ \mathbf{X}_2 & \mathbf{X}_1^H \end{bmatrix}, \tag{18}$$

where $\mathbf{X}_1$ and $\mathbf{X}_2$ are the symbol matrices as described in (15) and (16). That is, in the STC- OTFS scheme, the OTFS transmit vectors corresponding to $\mathbf{X}_1$ and $\mathbf{X}_2$ are transmitted from the first and the second antennas, respectively, during the first frame duration. During the second frame duration, the vectors corresponding to $-\mathbf{X}_2^H$ and $\mathbf{X}_1^H$ are transmitted from the first and second antennas, respectively. Now, it is important to look at the OTFS transmit vectors that are transmitted during the two frame duration. The OTFS transmit vector corresponding to the block $\mathbf{X}_k, k \in \{1,2\}$ in (18), denoted by $\mathbf{x}_k$, is nothing but the first row of $\mathbf{X}_k$. The transmitted vector corresponding to $\mathbf{X}_k^H, k \in \{1,2\}$, is the conjugate of the first column of $\mathbf{X}_k$. The vector corresponding to the first column of $\mathbf{X}_k$ can be obtained from $\mathbf{x}_k$ as $\hat{\mathbf{x}}_k = \mathbf{P}\mathbf{x}_k$, where $\mathbf{P}$ is $MN \times MN$ permutation matrix given by

$$\mathbf{P} = \mathbf{P}'_M \otimes \mathbf{P}'_N. \quad (19)$$

where $\mathbf{P}'_M \in \mathbb{R}^{M\times M}$ and $\mathbf{P}'_N \in \mathbb{R}^{N\times N}$ are left circulant matrices given by

$$\mathbf{P}'_M = \begin{bmatrix} 1 & 0 & \cdots 0 & 0 \\ 0 & 0 & \cdots 0 & 1 \\ 0 & 0 & \cdots 1 & 0 \\ \vdots & & & \\ 0 & 1 & \cdots 0 & 0 \end{bmatrix}_{M\times M} \quad \mathbf{P}'_N = \begin{bmatrix} 1 & 0 & \cdots 0 & 0 \\ 0 & 0 & \cdots 0 & 1 \\ 0 & 0 & \cdots 1 & 0 \\ \vdots & & & \\ 0 & 1 & \cdots 0 & 0 \end{bmatrix}_{N\times N}. \quad (20)$$

In general, $\hat{\mathbf{x}} = \mathbf{P}\mathbf{x}$ is of the form

$$\begin{aligned} \hat{\mathbf{x}} \;\; = \;\; & [x_0 \; x_{N-1} \; \cdots x_1 \; x_{(M-1)N} \; x_{MN-1} \cdots \\ & x_{((M-1)N)+1} \cdots x_N \; x_{2N-1} \cdots x_{N+1}]^T. \end{aligned} \quad (21)$$

It is interesting to note that the transmitted OTFS vectors in the second frame duration are not just the conjugated vectors, but are conjugated and permuted vectors of those transmitted in the first frame duration. Now, using (18) and the alternate representation of the MIMO-OTFS system in (17), the input-output equation of STC-OTFS can be written as

$$\begin{bmatrix} \mathbf{y}_1^T & \mathbf{y}_2^T \end{bmatrix} = \begin{bmatrix} \mathbf{h}'_1 & \mathbf{h}'_2 \end{bmatrix} \begin{bmatrix} \mathbf{X}_1 & -\mathbf{X}_2^H \\ \mathbf{X}_2 & \mathbf{X}_1^H \end{bmatrix} + \begin{bmatrix} \mathbf{v}_1^T & \mathbf{v}_2^T \end{bmatrix}, \quad (22)$$

where $\mathbf{y}_1$, $\mathbf{y}_2$ denote the $MN \times 1$ received vectors at the first and the second frame duration, respectively, $\mathbf{h}'_1$, $\mathbf{h}'_2$ denote the channel from the first and second antennas, respectively, and $\mathbf{v}_1$, $\mathbf{v}_2$ are $MN \times 1$ independent noise vectors.

To gain insight into the decoding complexity of this scheme, we consider MIMO-OTFS system model in (13). Denoting the channel matrices from the first and the second transmit antennas with $\mathbf{H}_1$ and $\mathbf{H}_2$, respectively, the received vectors in the first and second frame duration are

$$\mathbf{y}_1 = \mathbf{H}_1\mathbf{x}_1 + \mathbf{H}_2\mathbf{x}_2 + \mathbf{v}_1 \quad (23)$$
$$\mathbf{y}_2 = -\mathbf{H}_1(\hat{\mathbf{x}}_2)^* + \mathbf{H}_2(\hat{\mathbf{x}}_1)^* + \mathbf{v}_2. \quad (24)$$

At the receiver, permutation ($\mathbf{P}$) and conjugation are applied on $\mathbf{y}_2$. With this, we can write

$$\underbrace{\begin{bmatrix} \mathbf{y}_1 \\ (\hat{\mathbf{y}}_2)^* \end{bmatrix}}_{\triangleq\, \bar{\mathbf{y}}} = \underbrace{\begin{bmatrix} \mathbf{H}_1 & \mathbf{H}_2 \\ -\mathbf{H}_2^H & \mathbf{H}_1^H \end{bmatrix}}_{\triangleq\, \bar{\mathbf{H}}} \begin{bmatrix} \mathbf{x}_1 \\ \mathbf{x}_2 \end{bmatrix} + \begin{bmatrix} \mathbf{v}_1 \\ (\hat{\mathbf{v}}_2)^* \end{bmatrix}, \quad (25)$$

where $\hat{\mathbf{y}}_2$=$\mathbf{P}\mathbf{y}_2$ and $\hat{\mathbf{v}}_2 = \mathbf{P}\mathbf{v}_2$. Denoting $\bar{\mathbf{H}} = \begin{bmatrix} \mathbf{H}_1 & \mathbf{H}_2 \\ -\mathbf{H}_2^H & \mathbf{H}_1^H \end{bmatrix}$ as the effective channel matrix, we observe that the two block columns of $\bar{\mathbf{H}}$ are orthogonal. Therefore, the decoding problem for $\mathbf{x}_1$ and $\mathbf{x}_2$ can be decomposed into two separate orthogonal problems, thereby keeping the decoding complexity same as that of SISO-OTFS.

C. Diversity analysis

In this subsection, the asymptotic diversity of STC-OTFS scheme is analyzed. Let $\tilde{\mathbf{X}}_i$ and $\tilde{\mathbf{X}}_j$ be two distinct STC-OTFS codeword matrices and $\tilde{\mathbf{\Delta}}_{ij} \triangleq \tilde{\mathbf{X}}_i - \tilde{\mathbf{X}}_j$ be the difference matrix. The asymptotic diversity order of 2×1 STC-OTFS is defined as

$$\rho_{\text{STC-OTFS}} = \min\{\min_{i,j \;\; i\neq j} \text{rank}(\tilde{\mathbf{\Delta}}_{ij}), 2P\}. \quad (26)$$

We define the difference matrix corresponding to the kth independent OTFS symbol matrix as $\mathbf{\Delta}_{k,ij} = \mathbf{X}_{k,i} - \mathbf{X}_{k,j}$. Note that $\text{rank}(\tilde{\mathbf{\Delta}}_{ij}) = \text{rank}(\tilde{\mathbf{\Delta}}_{ij}^H \tilde{\mathbf{\Delta}}_{ij})$. Hence, we use $\tilde{\mathbf{\Delta}}_{ij}^H \tilde{\mathbf{\Delta}}_{ij}$ for analysis, which can be simplified as

$$\begin{aligned} \tilde{\mathbf{\Delta}}_{ij}^H \tilde{\mathbf{\Delta}}_{ij} &= \begin{bmatrix} \mathbf{\Delta}_{1,ij} & -\mathbf{\Delta}_{2,ij}^H \\ \mathbf{\Delta}_{2,ij} & \mathbf{\Delta}_{1,ij}^H \end{bmatrix}^H \begin{bmatrix} \mathbf{\Delta}_{1,ij} & -\mathbf{\Delta}_{2,ij}^H \\ \mathbf{\Delta}_{2,ij} & \mathbf{\Delta}_{1,ij}^H \end{bmatrix} \\ &= \begin{bmatrix} \mathbf{\Delta}_{1,ij}^H\mathbf{\Delta}_{1,ij} + \mathbf{\Delta}_{2,ij}^H\mathbf{\Delta}_{2,ij} & \mathbf{0}_{MN\times MN} \\ \mathbf{0}_{MN\times MN} & \mathbf{\Delta}_{1,ij}^H\mathbf{\Delta}_{1,ij} + \mathbf{\Delta}_{2,ij}^H\mathbf{\Delta}_{2,ij} \end{bmatrix}, \end{aligned} \quad (27)$$

Observe that $\tilde{\mathbf{\Delta}}_{ij}^H \tilde{\mathbf{\Delta}}_{ij}$ is block diagonal due to the commutative property of block circulant matrix with circulant blocks [12], and hence

$$\text{rank}(\tilde{\mathbf{\Delta}}_{ij}^H \tilde{\mathbf{\Delta}}_{ij}) = 2 \times \text{rank}(\mathbf{\Delta}_{1,ij}^H\mathbf{\Delta}_{1,ij} + \mathbf{\Delta}_{2,ij}^H\mathbf{\Delta}_{2,ij}). \quad (28)$$

It has been shown in [9] that the asymptotic diversity order of SISO-OTFS is one. Hence, the minimum rank of $\mathbf{\Delta}_{k,ij}$ is one $\forall\ k$. Now, consider the case when $\mathbf{\Delta}_{1,ij} = \mathbf{0}_{MN\times MN}$ and $\mathbf{\Delta}_{2,ij} = (a_1 - a_2)\mathbf{1}_{MN\times MN}$, where $a_1, a_2 \in \mathbb{S}$, where $\mathbb{S}$ is modulation alphabet (e.g., PSK/QAM), in which case the rank of $\mathbf{\Delta}_{1,ij}^H\mathbf{\Delta}_{1,ij} + \mathbf{\Delta}_{2,ij}^H\mathbf{\Delta}_{2,ij}$ is one. Therefore, the minimum rank of $\mathbf{\Delta}_{1,ij}^H\mathbf{\Delta}_{1,ij} + \mathbf{\Delta}_{2,ij}^H\mathbf{\Delta}_{2,ij}$ is one. Hence, from (26), as $P \geq 1$, the asymptotic diversity order of 2×1 STC-OTFS is two. Therefore, STC-OTFS can achieve an asymptotic diversity order of two. Extension of the system model in (22) to $2 \times n_r$ MIMO case, yields a diversity order of $2n_r$ with maximum likelihood (ML) detection while for the same case, MIMO-OTFS attains only n_r diversity.

Although STC-OTFS can extract full spatial diversity as discussed above, it fails to extract the delay-Doppler diversity offered by each link of the MIMO channel asymptotically. In [9], it has been shown that although the asymptotic diversity of SISO-OTFS modulation is one, it exhibits higher order diversity in the finite SNR regime, for increased OTFS frame sizes. This is true in the case of STC-OTFS system as well (as will be seen through simulations in Sec. IV). However, for low-latency applications which use small frame sizes, we propose the use of STC-OTFS with phase rotation to extract the full delay-Doppler diversity as well. In the next subsection, we show that, using phase rotation scheme for the STC-OTFS, full spatial and delay-Doppler diversity can be achieved.

D. Phase rotation in STC-OTFS

In this subsection, we consider STC-OTFS with phase rotation. We use Theorem 1 in [9], which is restated as follows.

Theorem 1. *Let*

$$\mathbf{\Phi} = \text{diag}\left\{\phi_0, \phi_1, \cdots, \phi_{MN-1}\right\} \tag{29}$$

be the phase rotation matrix and $\mathbf{x}' = \mathbf{\Phi}\mathbf{x}$ be the phase rotated OTFS transmit vector. SISO-OTFS with the above phase rotation achieves the full diversity when $\phi_i = e^{ja_i}$, $i = 0, 1, \cdots, MN-1$, are transcendental numbers with $a_i \neq 0$, real, distinct and algebraic.

In STC-OTFS, we multiply the OTFS transmit vector from each of n_t transmit antennas during every frame duration by a diagonal phase rotation matrix $\mathbf{\Phi}$ of the form (29). Let the difference matrix of phase rotated STC-OTFS codeword matrix be denoted with $\tilde{\mathbf{\Delta}}_{ij}^{\phi}$. The asymptotic diversity of 2×1 phase rotated STC-OTFS can be defined similar to (26) as

$$\rho_{\text{STC-OTFS}} = \min\{\min_{i,j \ \ i\neq j} \ \text{rank}(\tilde{\mathbf{\Delta}}_{ij}^{\phi}), 2P\}. \tag{30}$$

We denote the difference matrix corresponding to the kth phase rotated OTFS symbol matrix with $\mathbf{\Delta}_{k,ij}^{\phi}$. Now, as a consequence of Theorem 1, $\mathbf{\Delta}_{k,ij}^{\phi}$ has a full rank of MN for all k. As described in the previous subsection, the minimum rank of $\tilde{\mathbf{\Delta}}_{ij}^{\phi}$ is same as that of $(\tilde{\mathbf{\Delta}}_{ij}^{\phi})^H\tilde{\mathbf{\Delta}}_{ij}^{\phi} = 2\times \text{rank}((\mathbf{\Delta}_{1,ij}^{\phi})^H\mathbf{\Delta}_{1,ij}^{\phi} + (\mathbf{\Delta}_{2,ij}^{\phi})^H\mathbf{\Delta}_{2,ij}^{\phi})$. Now, for any two distinct codewords ($\tilde{\mathbf{\Delta}}_{ij}^{\phi} \neq \mathbf{0}$), either $\mathbf{\Delta}_{1,ij}^{\phi} \neq \mathbf{0}$ or $\mathbf{\Delta}_{2,ij}^{\phi} \neq \mathbf{0}$ or both are non-zero matrices. If $\mathbf{\Delta}_{k,ij}^{\phi} \neq \mathbf{0}$, from Theorem 1, it will be full rank. Thus, at least one of $(\mathbf{\Delta}_{1,ij}^{\phi})^H\mathbf{\Delta}_{1,ij}^{\phi}$or $(\mathbf{\Delta}_{2,ij}^{\phi})^H\mathbf{\Delta}_{2,ij,}^{\phi}$ or both are positive definite matrices. Therefore, their sum $(\mathbf{\Delta}_{1,ij}^{\phi})^H\mathbf{\Delta}_{1,ij}^{\phi}+(\mathbf{\Delta}_{2,ij}^{\phi})^H\mathbf{\Delta}_{2,ij}^{\phi}$ is also positive definite, and hence $\tilde{\mathbf{\Delta}}_{ij}^{\phi}$ has full rank of $2MN$ for any input symbols. Since $P \leq MN$, the asymptotic diversity order of 2×1 phase rotated STC-OTFS is $2P$. Extension of this scheme to $2 \times n_r$ MIMO case yields a diversity order of $2Pn_r$ with ML detection.

IV. Simulation Results

In this section, we present the BER performance of STC-OTFS and STC-OTFS with phase rotation.

Performance of STC-OTFS system: Figure 3 shows the BER performance of $i)$ SISO-OTFS, $ii)$ 2×1 STC-OTFS, and $iii)$ 2×2 STC-OTFS systems. All the systems use $M = N = 2$, $P = 2$, BPSK modulation, and ML detection. A carrier frequency of 4 GHz and a subcarrier spacing of 3.75 kHz are considered. The parameters considered for the simulations are given in Table I. The channel model considered for simulations is described in Sec.II-C and the delay and Doppler values used are as per Table I. From Fig. 3, it is observed that the simulated BER for 2×1 and 2×2 STC-OTFS systems show diversity orders of two and four, respectively, verifying the analytical diversity order derived in Sec. III.

Figure 4 shows the BER performance of $i)$ SISO-OTFS, $ii)$ 2×1 STC-OTFS, and $iii)$ 2×2 STC-OTFS systems for

Parameter	Value
Carrier frequency (GHz)	4
Subcarrier spacing (kHz)	3.75
Frame sizes	$M = N = 2$, $M = 4, N = 2$
MIMO configurations	1×1, 2×1, 2×2
Delay-Doppler profile for $P = 2$ (τ_i (μs), ν_i (kHz))	(0,0), (133.3,1.875)
Delay-Doppler profile for $P = 4$ (τ_i (μs), ν_i (kHz))	(0,0), (0,1.875), (133.3,0), (133.3,1.875)
Maximum speed (km/h)	506.2
Modulation scheme	BPSK

TABLE I: Simulation parameters.

an $M = 4$, $N = 2$ and $P = 2$. All the systems use BPSK modulation and ML detection. Other parameters considered for the simulations are given in Table I. From Fig. 4, it can observed that the simulated BER performance for all the systems with $M = 4$ and $N = 2$ outperforms the systems with $M = N = 2$ in Fig. 3. This illustrates that the STC-OTFS systems with increased frame size can potentially offer better diversity orders in the finite SNR regime before attaining its asymptotic diversity of $2n_r$.

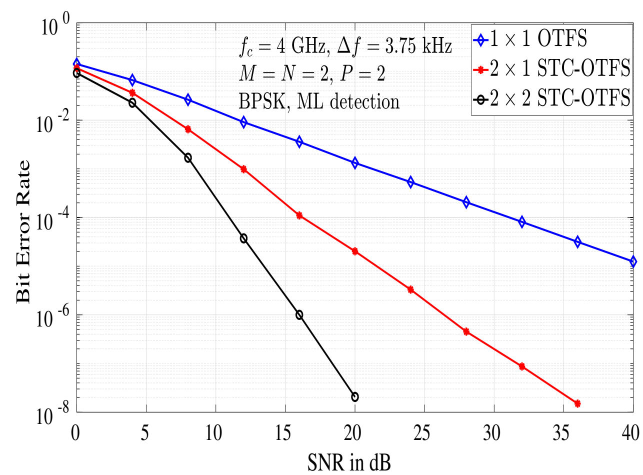

Fig. 3: BER performance of $i)$ 1×1 OTFS, $ii)$ 2×1 STC-OTFS, and $iii)$ 2×2 STC-OTFS for $M = N = 2$.

Performance of STC-OTFS with phase rotation: Figure 5 shows the BER performance of STC-OTFS with phase rotation in a 2×1 MIMO system with $i)$ $P = 2$ and $ii)$ $P = 4$. For comparison, we also plot the BER performance of STC-OTFS without phase rotation. All the systems use $M = N = 2$ and BPSK modulation. Other parameters are given in Table I. For the simulations, the phase rotation matrix, $\mathbf{\Phi} = \text{diag}\{1, e^{j\frac{1}{MN}} \cdots e^{j\frac{MN-1}{MN}}\}$ is used. From Fig. 4, we observe that the STC-OTFS with phase rotation achieves better diversity order compared to STC-OTFS. Specifically, 2×1 phase rotated STC-OTFS system achieves a diversity order of $2P$, whereas STC-OTFS achieves a diversity of two. This demonstrates that the phase rotated STC-OTFS can achieve full spatial and delay-Doppler diversity of $2n_rP$ in $2 \times n_r$ MIMO channels. Though STC-OTFS without phase rotation can exhibit close to full spatial and delay-Doppler diversity in the finite SNR regime for large frame sizes, STC-OTFS

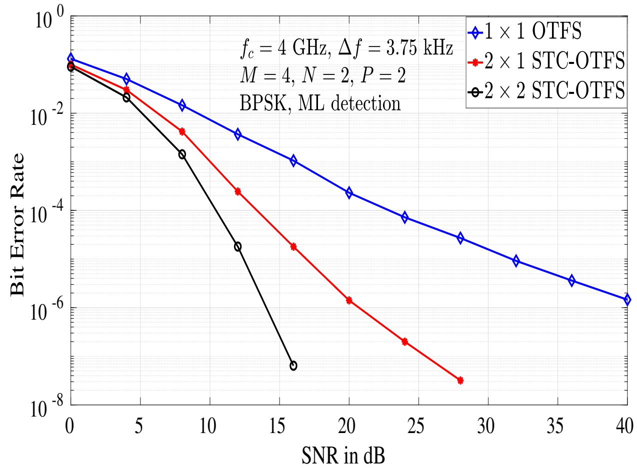

Fig. 4: BER performance of $i)$ 1×1 OTFS, $ii)$ 2×1 STC-OTFS, and $iii)$ 2×2 STC-OTFS for $M = 4, N = 2$.

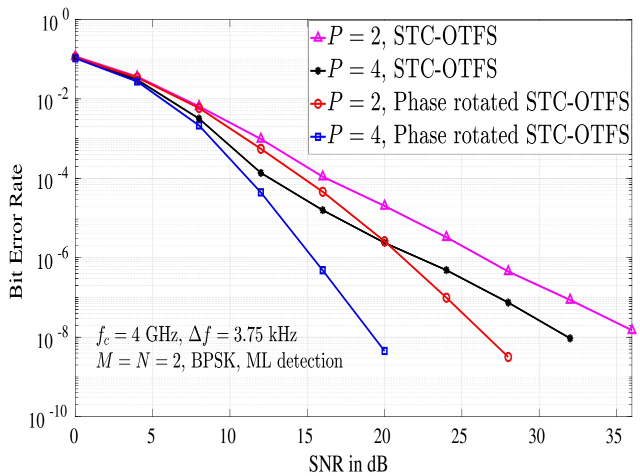

Fig. 5: BER performance of 2×1 STC-OTFS with and without phase rotation for $i)$ $P = 2$ and $ii)$ $P = 4$.

with phase rotation achieves full diversity even for small frame sizes. This makes it attractive for low latency applications that use small frame sizes for low decoding delays.

V. Conclusions

In this work, we proposed the use of space-time coding in OTFS modulation. We formulated the construction of a space-time code based on Alamouti code structure in a matrix form for OTFS. We proved analytically that the full spatial transmit diversity order of two is achieved in a 2×1 STC-OTFS system. We also showed that the proposed space-time code along with the phase rotation can achieve the full spatial and delay-Doppler diversity of $2P$ in a 2×1 STC-OTFS system. The STC-OTFS scheme with phase rotation in a $2\times n_r$ system can yield a diversity order of $2Pn_r$. Simulation results on the BER performance validated the analytically predicted diversity orders. We further note that the STC-OTFS with phase rotation is of practical interest as it can achieve good diversity performance even with small frame sizes making it suited for low-latency applications.

References

[1] R. Hadani, S. Rakib, M. Tsatsanis, A. Monk, A. J. Goldsmith, A. F. Molisch, and R. Calderbank, "Orthogonal time frequency space modulation," *Proc. IEEE WCNC'2017*, pp. 1-7, Mar. 2017.

[2] R. Hadani and A. Monk, "OTFS: A new generation of modulation addressing the challenges of 5G," online: arXiv:1802.02623 [cs.IT] 7 Feb 2018.

[3] R. Hadani, S. Rakib, S. Kons, M. Tsatsanis, A. Monk, C. Ibars, J. Delfeld, Y. Hebron, A. J. Goldsmith, A. F. Molisch, and R. Calderbank, "Orthogonal time frequency space modulation," online: arXiv:arXiv:1808.00519v1 [cs.IT] 1 Aug 2018.

[4] R. Hadani, S. Rakib, A. F. Molisch, C. Ibars, A. Monk, M. Tsatsanis, J. Delfeld, A. Goldsmith, and R. Calderbank, "Orthogonal time frequency space (OTFS) modulation for millimeter-wave communications systems," *Proc. IEEE MTT-S Intl. Microwave Symp.*, pp. 681-683, Jun. 2017.

[5] A. Farhang, A. R. Reyhani, L. E. Doyle, and B. Farhang-Boroujeny, "Low complexity modem structure for OFDM-based orthogonal time frequency space modulation," *IEEE Wireless Commun. Lett.*, vol. 7, no. 3, pp. 344-347, June 2018.

[6] P. Raviteja, K. T. Phan, Y. Hong, and E. Viterbo, "Interference cancellation and iterative detection for orthogonal time frequency space modulation," *IEEE Trans. Wireless Commun*, vol. 17, no. 10, pp. 6501-6515, Oct. 2018.

[7] K. R. Murali and A. Chockalingam, "On OTFS modulation for high-Doppler fading channels," *Proc. ITA'2018*, San Diego, Feb. 2018.

[8] M. K. Ramachandran and A. Chockalingam, "MIMO-OTFS in high-Doppler fading channels: signal detection and channel estimation," accepted in *IEEE GLOBECOM'2018*, Dec. 2018. Online: arXiv:1805.02209v1 [cs.IT] 6 May 2018.

[9] G. D. Surabhi, R. M. Augustine, and A. Chockalingam, "On the diversity of OTFS modulation in doubly-dispersive channels," Online: arXiv:1808.07747 [sc.IT] 23 Aug 2018.

[10] D. N. Dao and C. Tellambura, "Capacity-approaching semi-orthogonal space-time block codes," *Proc. IEEE GLOBECOM'2005*, Nov. 2005.

[11] S. M. Alamouti, "A simple transmit diversity technique for wireless communications, "*IEEE Journal on selected areas in communications*, vol. 16, no. 8, pp. 1451-1458, Oct. 1998.

[12] P. J. Davis, *Circulant Matrices*, American Mathematical Society, 2012.